AGU PUBLICATIONS

Geophysical Research Letters

Rapid changes in biomass burning aerosols by atmospheric oxidation

Ville Vakkari[1,2], Veli-Matti Kerminen[1], Johan Paul Beukes[3], Petri Tiitta[3,4], Pieter G. van Zyl[3], Miroslav Josipovic[3], Andrew D. Venter[3], Kerneels Jaars[3], Douglas R. Worsnop[1,5], Markku Kulmala[1], and Lauri Laakso[2,3]

[1]Department of Physics, University of Helsinki, Helsinki, Finland, [2]Research and Development, Finnish Meteorological Institute, Helsinki, Finland, [3]Unit for Environmental Sciences and Management, North-West University, Potchefstroom, South Africa, [4]Department of Environmental Science, University of Eastern Finland, Kuopio, Finland, [5]Center for Aerosol and Cloud Chemistry, Aerodyne Research, Inc., Billerica, Massachusetts, USA

Abstract Primary and secondary aerosol particles originating from biomass burning contribute significantly to the atmospheric aerosol budget and thereby to both direct and indirect radiative forcing. Based on detailed measurements of a large number of biomass burning plumes of variable age in southern Africa, we show that the size distribution, chemical composition, single-scattering albedo, and hygroscopicity of biomass burning particles change considerably during the first 2–4 h of their atmospheric transport. These changes, driven by atmospheric oxidation and subsequent secondary aerosol formation, may reach a factor of 6 for the aerosol scattering coefficient and a factor >10 for the cloud condensation nuclei concentration. Since the observed changes take place over the spatial and temporal scales that are neither covered by emission inventories nor captured by large-scale model simulations, the findings reported here point out a significant gap in our understanding on the climatic effects of biomass burning aerosols.

1. Introduction

Biomass burning is considered to be the largest source of primary carbonaceous aerosol particles and a major source of reactive trace gases into the Earth's atmosphere [*Andreae and Merlet*, 2001; *van der Werf et al.*, 2010; *Akagi et al.*, 2011; *Mao et al.*, 2013; *Yokelson et al.*, 2013]. The climatic effects of biomass burning particles have remained poorly quantified since their optical and cloud activating properties are very diverse, and depend in a complex manner on the fuel type, combustion phase, and environmental conditions, as well as on atmospheric aging of emitted particles and trace gases [*Reid et al.*, 2005a; *Andreae and Rosenfeld*, 2008; *Janhäll et al.*, 2010; *Spracklen et al.*, 2011; *Engelhart et al.*, 2012; *Lack et al.*, 2012, 2013; *Bond et al.*, 2013; *Liu et al.*, 2013].

Our understanding of biomass burning aerosols relies largely on emission factors obtained from laboratory experiments and field measurements conducted in the immediate vicinity of fires [*van der Werf et al.*, 2010; *Akagi et al.*, 2011; *Yokelson et al.*, 2013]. Much less information is available on atmospheric aging of biomass burning emissions. However, studies performed in individual biomass burning plumes and in the laboratory indicate potential large changes in the size distribution and chemical composition of biomass burning particles during their atmospheric transport [*Reid et al.*, 2005a; *Capes et al.*, 2008; *Hennigan et al.*, 2011, 2012]. The overall picture of these changes has, though, remained heterogeneous. Some studies indicate increasing aerosol mass or number concentration [*Hobbs et al.*, 2003; *Grieshop et al.*, 2009a; *Yokelson et al.*, 2009; *Hennigan et al.*, 2011, 2012], but there are also observations of little or no secondary aerosol formation [*Capes et al.*, 2008; *Akagi et al.*, 2012].

On a global scale, central and southern Africa form one of the largest sources of biomass burning aerosols [*Langmann et al.*, 2009; *van der Werf et al.*, 2010]. Here we have compiled measurements from 60 individual biomass burning plumes observed in South Africa. To our knowledge, this is the first data set of atmospheric observations that facilitates studying the time evolution of biomass burning plume aerosol size distribution including the ultrafine size range. Furthermore, this data set includes a large number of plumes transported in nighttime, enabling comparison of the plume evolution with and without photochemical reactions [cf. *Adler et al.*, 2011]. The large data set enables also studying the effect of varying emissions, as characterized by the ratio of flaming to smoldering at the fire, to the plume evolution. Our results indicate rapid changes in the

biomass burning aerosol during the first few hours of atmospheric transport. For instance, the emission of cloud condensation nuclei (CCN) may increase by more than a factor of 10 in 2 h depending on atmospheric oxidation and the initial emissions.

2. Materials and Methods

Measurements were carried out from 20 May 2010 to 15 April 2012 in South Africa at the Welgegund measurement station (www.welgegund.org), which is located approximately 100 km southwest from Johannesburg (26.57°S 26.94°E, 1480 m above sea level). The Welgegund measurement station is located on a privately owned farm in the Dry Highveld Grassland bioregion, which covers approximately a third of the surface of South Africa. Welgegund can be considered as a background location with very few local anthropogenic sources. The distance to the nearest blacktop road is 10 km and to the nearest town 30 km. Approximately 100 km to the north of Welgegund the vegetation type changes into savannah, while approximately 200 km to the west of Welgegund the vegetation type changes into open shrublands [*Friedl et al.*, 2002].

At the Welgegund station, the aerosol number size distribution from 12 to 840 nm was measured with a differential mobility particle sizer (DMPS) at a time resolution of 9 min. Aerosol absorption was measured with a Thermo model 5012 multiangle absorption photometer, which was used also to estimate the black carbon (BC) concentration. Aerosol scattering was measured with a three-wavelength nephelometer (Ecotech Aurora 3000) from January 2011. The aerosol chemical composition for nonrefractive compounds was measured at a 30 min time resolution with an Aerodyne aerosol chemical speciation monitor (ACSM) [*Ng et al.*, 2011] for a 1 year period from September 2010 to August 2011. Of the gas phase species carbon monoxide (CO) was measured with a Horiba APMA-360 analyzer and ozone (O_3) with an Environment s.a. 41M analyzer. For a more detailed description of the instrumentation, we refer the reader to the supporting information and to *Petäjä et al.* [2013].

Identification of biomass burning plume periods in the Welgegund measurements was based on a combination of remote-sensing observations from the Moderate Resolution Imaging Spectroradiometer (MODIS) collection 5 burned area product [*Roy et al.*, 2008] and local measurements of CO, BC, and aerosol particle concentrations. A measurement period was identified by visual inspection as a biomass burning plume if there was at least a 40 ppb increase in the CO concentration in the 15 min averaged data, simultaneous increases in the BC and aerosol particle concentrations, and if the MODIS burned area product indicated burned areas along the path of the air mass arriving at Welgegund. Only instances when the fire-generated aerosol could be clearly separated from the preexisting aerosol were considered. The preceding 30 min median was considered to best represent the preexisting aerosol background and it was used to calculate the excess concentration, which is denoted with a Δ throughout the paper.

The age of the plume was calculated from the distance from the fire to the measurement station, when the location of the fire was established with the assumption that the plume had traveled at the mean wind speed measured at Welgegund [cf. *Akagi et al.*, 2012]. The plume age was calculated separately for each size distribution and chemical composition measurement during the plume by taking into account the time resolution for each instrument, i.e., for the size distribution wind speed had a 9 min mean, while the chemical composition had a 30 min mean. For plumes with unclear origin, the minimum age was estimated from the distance to the nearest fire upwind of the site. However, this estimate was not used beyond identifying plumes older than 2 h. Additionally, the age of the plume was estimated only if the mean wind speed was at least 0.5 m s^{-1}. Such low wind speeds occurred only during the nighttime.

The plume measurements were divided into daytime and nighttime based on the age of the plume and the measured global radiation. A measurement was considered to represent pure daytime conditions if during the age of the plume the measured global radiation at Welgegund was continuously above 100 W m^{-2}. Correspondingly, pure nighttime plumes were defined as global radiation being continuously below 30 W m^{-2} during the age of the plume. Forty-eight percent of the in-plume measurements could be categorized as pure nighttime and 17% as pure daytime observations.

The location of the fire could be identified for 33 of the 60 plumes observed, while for the remaining 27 plumes, there were several possible fires upwind of the measurement site. The known fire locations were combined with MODIS collection 5 yearly land cover type product for 2011 [*Friedl et al.*, 2002, 2010; *Belward et al.*, 1999;
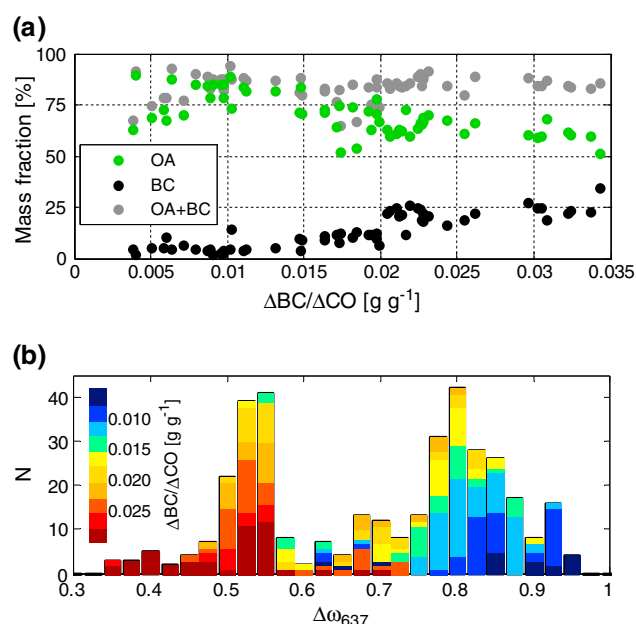
Figure 1. BC emission affects the ratio of organic aerosol to BC mass fraction and the single-scattering albedo in biomass burning plumes. (a) Organic aerosol (OA) and black carbon (BC) mass fractions in plumes older than 2 h. OA mass fraction has a significant negative correlation ($R = -0.68$, $P = 3e-9$) with NEMR of BC. (b) The frequency distribution of the aerosol single-scattering albedo, $\Delta\omega$, for all the plumes measured. Different colors indicate different values of the NEMR of BC. Here N indicates the number of 9 min in-plume samples for each $\Delta\omega$.

Scepan, 1999]. According to the International Geosphere-Biosphere Program (IGBP) classification, approximately 30% of the known fire locations were in savannas and another 30% were in grasslands. The remaining 40% of the known fire locations were a mixture of either cropland and savanna, or cropland and grassland vegetation types, indicating that probably a large fraction of the observed plumes originated in agricultural burning. It is typical for agricultural burnings in southern Africa that the fire is started in the evening and a similar pattern has been observed also in other cropland regions, e.g., in Brazil [*Giglio*, 2007]. This, together with less mixing and thus less dilution in nighttime, may explain the large fraction of nighttime plumes at Welgegund.

The plumes observed at Welgegund had been traveling in the surface layer for an average (median) of 2.4 h, which is such a long period that due to CO_2 exchange with vegetation the uncertainties associated with the ΔCO_2 determined at Welgegund are too high to be used in emission factor calculations [e.g., *Akagi et al.*, 2011]. Therefore, the extensive aerosol properties presented here were scaled with ΔCO, i.e., as normalized excess mixing ratio (NEMR) with respect to CO. However, the NEMR of BC, $\Delta BC/\Delta CO$, can be used as a measure of burning conditions (i.e., the ratio of smoldering to flaming). An increasing $\Delta BC/\Delta CO$ value is indicative of increasing flaming fraction during the burning [*Yokelson et al.*, 2009]. The NEMR was defined for DMPS-derived quantities only if ΔCO was at least 40 ppb (9 min mean) and for ACSM-derived quantities if ΔCO was at least 20 ppb (30 min mean). All NEMRs were calculated separately for each size distribution or a corresponding 9 min time period, i.e., not averaged over a plume.

A more detailed description of the methods can be found in the supporting information.

3. Results and Discussion

Carbonaceous aerosol, i.e., organic aerosol (OA) and BC, constituted on average 85% of the submicron aerosol mass in the aged (older than 2 h) biomass burning plumes (Figure 1a). Furthermore, the partitioning between OA and BC was dependent on the ratio of flaming to smoldering combustion (Figure 1a), which is in good agreement with laboratory studies [*Christian et al.*, 2003; *Liu et al.*, 2013]. On the other hand, emissions of many volatile organic compounds (VOCs) decrease with increasing fraction of flaming combustion [e.g., *Yokelson et al.*, 2013, and references therein], which implies that the concentration of secondary organic aerosol precursors will be lower in high $\Delta BC/\Delta CO$ conditions. Allowing time for oxidation and secondary aerosol formation, this leads to a lower OA fraction at higher $\Delta BC/\Delta CO$, which is consistent with what we observed in Figure 1a. Lower concentrations of secondary organic aerosol precursors will also lead to smaller changes in the aerosol size distribution and optical properties during the plume aging.

The aerosol single-scattering albedo calculated from excess scattering and absorption ($\Delta\omega$, see supporting information for details) had a distinct bimodal distribution (Figure 1b) depending on the $\Delta BC/\Delta CO$ ratio, except for the intermediate values of this ratio for which $\Delta\omega$ spread over both modes (Figure 1b). The values of $\Delta\omega$ in the "bright" mode (0.81 ± 0.06) are comparable to those measured by other investigators for grass or
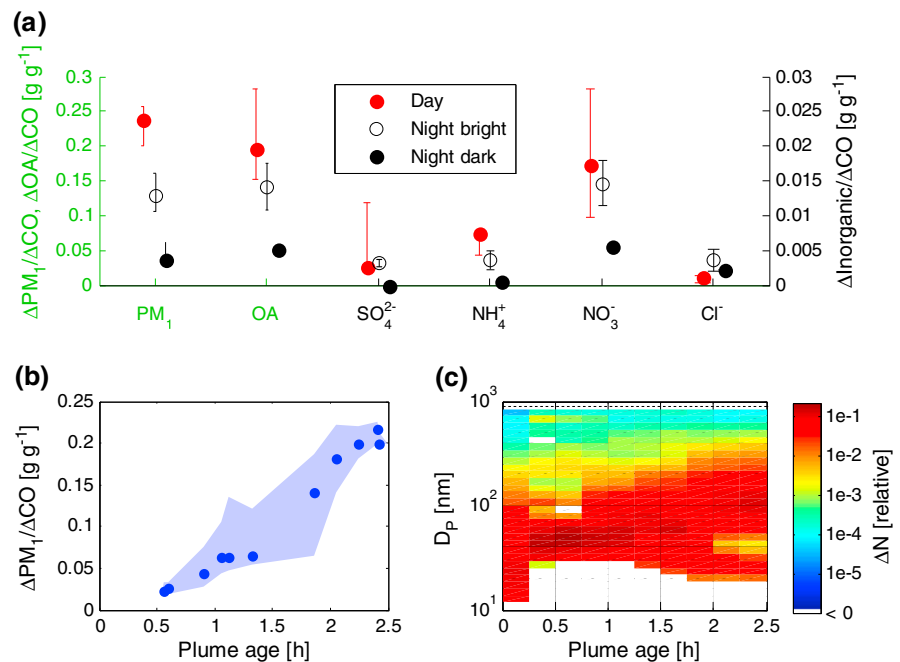
Figure 2. Secondary aerosol formation is increased in daytime plumes. All graphs are for $\Delta BC/\Delta CO < 0.015$ g g^{-1}. (a) NEMRs of different aerosol constituents in daytime and nighttime plumes. The dots and range represent the median values with upper and lower quartiles. The differences in NEMR are indicative of more efficient secondary production (PM$_1$ mass, OA, SO$_4^{2-}$, NH$_4^+$, and NO$_3^-$) or loss (Cl$^-$) of secondary particulate matter during daytime than during nighttime, as well as between different types of nighttime plumes. The loss of Cl$^-$ can be explained by the reaction of potassium chloride, a typical primary aerosol species in biomass burning aerosols, with stronger acids during the plume aging [*Akagi et al.*, 2012]. (b) Time evolution of NEMR of daytime PM$_1$, calculated from measured aerosol volume concentrations by assuming a particle density of 1.5 g/cm^3 (cf. supporting information). The dots represent 45 min running median values with respect to the plume age and the shaded area covers the upper and lower quartiles of the values. (c) Time evolution of the daytime aerosol size distribution plotted as 45 min running median with respect to the plume age.

savanna fires [*Reid et al.*, 2005b; *Leahy et al.*, 2007], but the values of $\Delta\omega$ in the "dark" mode (0.57 ± 0.06) are very low and have only rarely been observed in the atmosphere [*Reid and Hobbs*, 1998] or in laboratory studies [*Chen et al.*, 2006; *Lewis et al.*, 2008; *Liu et al.*, 2013]. Grassland surface albedo is typically 0.2 [e.g., *Gao et al.*, 2005], and hence, the critical single-scattering albedo, i.e., the limit value between cooling and heating direct aerosol effect [e.g., *King et al.*, 1999], is approximately 0.7. The value of $\Delta\omega$ in the dark mode was clearly smaller than 0.7, which implies that in these cases, the biomass burning aerosol was having a heating effect, at least over the grassland. In fresh plumes (plume age less than 0.5 h), the aerosol size distribution and optical properties were connected closely with $\Delta BC/\Delta CO$, i.e., with burning conditions (Figure S1 in the supporting information), which is in good agreement with laboratory experiments [*Chen et al.*, 2006; *Liu et al.*, 2013]. We therefore segregated the measurement data into a few $\Delta BC/\Delta CO$ bins before investigating the effects of plume aging.

We observed an increase in $\Delta\omega$ during the plume aging [cf. *Abel et al.*, 2003], for $\Delta BC/\Delta CO$ ranging from 0.01 to 0.025 g g^{-1}, which covers 60% of in-plume observations at Welgegund (Figure S8). The higher the $\Delta BC/\Delta CO$ was, the slower was the increase rate in $\Delta\omega$ (Figure S2). For instance, in the 0.0125 to 0.0175 g g^{-1} $\Delta BC/\Delta CO$ bin, $\Delta\omega$ increased from 0.55 to 0.8 in 1 h, which compares nicely with ω increasing from 0.75 to 0.90 in 40 min ($\Delta BC/\Delta CO \approx 0.007$ g g^{-1}) in a single biomass burning plume in the Yucatan [*Yokelson et al.*, 2009]. However, in cases where the plume had been transported during the nighttime and exposed to weak vertical mixing conditions, $\Delta\omega$ remained in the dark mode even after 2 h and for $\Delta BC/\Delta CO < 0.02$ g g^{-1} (Figure S3). Therefore, dark $\Delta\omega$ and $\Delta BC/\Delta CO < 0.02$ g g^{-1} can be used to identify unprocessed aerosol in nighttime data, which turns out to be a valuable tool in understanding the variability in aged nighttime plumes (cf. Figure 2a).

Atmospheric aging processes influenced not only $\Delta\omega$ but also aerosol scattering properties. We found that the NEMR of the aerosol scattering coefficient increased by a factor of up to 6 during the first 2 h of transport
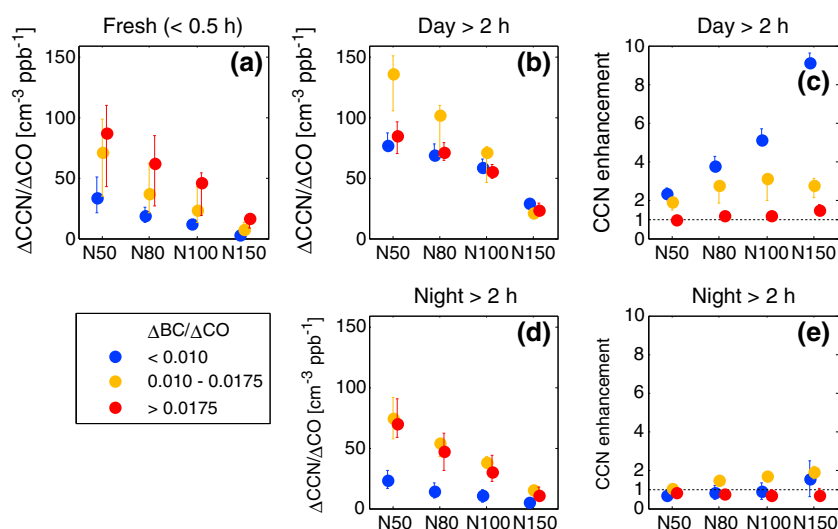
Figure 3. The NEMRs of CCN-sized particles (a) in fresh plumes, (b) in aged (> 2 h) daytime plumes, and (d) in aged nighttime plumes, together with the CCN enhancement ratio caused by plume aging (c) in daytime plumes and (e) in nighttime plumes. The total number concentration of particles larger than a certain threshold diameter (50, 80, 100, or 150 nm) was used as a proxy for the CCN concentration that is in line with typical minimum diameters of atmospheric aerosol particles capable of cloud droplet activation [*Kerminen et al.*, 2012]. During daytime, the CCN concentrations (NEMR) were increased in most of the plumes (and threshold particle sizes), with the exception of high $\Delta BC/\Delta CO$ aerosol associated with high primary CCN concentrations. During nighttime, however, the NEMR of CCN increases only in a minor fraction of the plumes. The dots and range represent the median values with upper and lower quartiles.

time (Figure S4). This increase was more pronounced at shorter wavelengths and lower values of $\Delta BC/\Delta CO$. A similar increase in the aerosol scattering NEMR at 530 nm wavelength has been reported for a single plume in California, where a factor of 2.5 increase was observed during 4 h of atmospheric aging [*Akagi et al.*, 2012].

We observed a steep increase in the submicron aerosol volume-derived PM$_1$ NEMR during the first 2 h of aging in daytime plumes with $\Delta BC/\Delta CO < 0.015$ g g^{-1} (Figure 2). This is in agreement with previous observations on formation of secondary inorganic, and sometimes organic, particulate matter in biomass burning plumes [*Yokelson et al.*, 2009; *Akagi et al.*, 2012]. Furthermore, in plumes that had undergone at least 2 h of aging, the NEMR of both organic and inorganic aerosol were clearly the highest in daytime plumes, i.e., in plumes that were influenced by photochemical reactions. The NEMR of aged daytime OA was higher by a factor of 4 than the NEMR of nighttime dark (i.e., unprocessed) OA (Figure 2a), which is reasonably close to laboratory experiments that have reported OA enhancement ratios of 2–3 as a result of photochemical processing [*Grieshop et al.*, 2009a; *Hennigan et al.*, 2011].

In some of the youngest samples, the total particle number concentration exceeded 100,000 cm^{-3}, which means that coagulation was able to influence both particle growth and particle number concentration [*Kerminen et al.*, 2004]. In most cases, however, the estimated time scales over which coagulation modifies the particles number size distribution exceeded 10 h, which is much less than the corresponding time scales for condensational growth. We conclude that coagulation was important in only the very near-source evolution of the plume. The dominance of secondary aerosol formation (via condensation) compared to coagulation becomes also clear when comparing nighttime plumes to daytime plumes. Coagulation should be as effective during the night as during the day, or even more effective during the night due to weaker mixing conditions, so the much more pronounced changes observed during the daytime (cf. Figures 3 and S4 and Table S2) clearly indicate the dominance of condensation over coagulation.

In the nighttime plumes, $\Delta\omega$ and particulate nitrate (NO$_3^-$) NEMR correlated positively with the O$_3$ concentration (Figure S5). This suggests that the nighttime oxidation reactions affecting aerosol properties were most likely initiated by O$_3$, probably through the nitrate radical (NO$_3^\bullet$) formation from the O$_3$ reaction with NO$_2$. Secondary aerosol formation in the absence of UV radiation has been observed also in some laboratory experiments, but only if O$_3$ is present [e.g., *Grieshop et al.*, 2009a]. The organic and inorganic mass NEMRs were higher after 2 h in the bright nighttime plumes compared to the dark plumes, but lower than in

the daytime plumes. This suggests that the secondary aerosol formation in biomass burning plumes depends not only on the emissions but also crucially on atmospheric oxidation mechanisms during the plume transport.

We found that the organic particulate material was, on average, much less oxidized in the dark nighttime plumes compared to the bright nighttime plumes or daytime plumes, as indicated by the oxygen to carbon ratio estimated from the ACSM measurements (Figure S6). This is in good agreement with previous observations on the aging of biomass burning aerosol [*Capes et al.*, 2008; *Grieshop et al.*, 2009b; *Cubison et al.*, 2011; *Hennigan et al.*, 2011; *Ortega et al.*, 2013]. The major increase in the oxygen to carbon ratio implies a significant increase in the hygroscopicity [*Massoli et al.*, 2010] of biomass burning aerosol during the initial stage of aging.

In order to obtain insight into the production of CCN in biomass burning plumes, we investigated differences in aerosol number size distributions between plumes of different atmospheric transport times. Visually, the differences were most apparent for fresh daytime plumes in the $\Delta BC/\Delta CO < 0.015$ range that showed clear signs of new particle formation and growth (Figure 2c), as well as a simultaneous increase in the aerosol particle count mean diameter (Figure S7) and mass (Figure 2b). Laboratory experiments combined with model simulations suggest that new particle formation in biomass burning plumes contributes significantly to the global CCN budget [*Hennigan et al.*, 2011, 2012]. We found that the daytime plumes produced new CCN and that this production seemed to be more efficient in plumes with lower NEMR of BC, i.e., in plumes having lower concentrations of primary CCN (Figures 3 and S1). The factor by which CCN concentrations in terms of their NEMR increased during the plume aging reached levels as high as 9—the increase being higher when assuming a larger minimum size limit for CCN. The increasing hygroscopicity of particles during the plume aging decreases the diameter threshold for CCN activation. In our case, this alone can increase the NEMR of CCN by as much as a factor of 1.6, as indicated in the supporting information. As a result, the total increase in the NEMR of CCN during the initial aging may reach a factor larger than 10.

Previous measurement campaigns in southern Africa [*Le Canut et al.*, 1996; *Formenti et al.*, 2003] give a range of 10 to 30 cm^{-3} ppb^{-1} for the NEMR of particles larger than 100 nm ($\Delta N100/\Delta CO$), which is in good agreement with our observations for fresh plumes with low and moderate $\Delta BC/\Delta CO$, i.e., $\Delta BC/\Delta CO < 0.010$ and $\Delta BC/\Delta CO$ 0.010–0.0175, respectively (see Figure 3a and Table S1). However, $\Delta N100/\Delta CO$ exceeding 45 cm^{-3} ppb^{-1} as observed for $\Delta BC/\Delta CO > 0.0175$ (cf. Figure 3a and Table S1) exceed the current mean estimates by a factor of 2 [*Janhäll et al.*, 2010]. Such high $\Delta N100/\Delta CO$ values have been reported previously only very rarely [*Le Canut et al.*, 1996].

4. Concluding Remarks

Based on detailed measurements of 60 biomass burning plumes in southern Africa, we have shown that the climatically most important properties of biomass burning aerosols change rapidly and to a substantial degree during their initial atmospheric transport in most plumes. We have further shown that these changes can be tied in a consistent manner to atmospheric oxidation chemistry and subsequent evolution of the particle number size distribution and chemical composition in aging plumes. Our analysis indicates that approximately two thirds of the biomass burning plume aerosol that we observed in a large sample size in southern Africa has the potential for significant, by at least of factor of 2, increase in the number of CCN during the initial 2–4 h of the plume transport in the atmosphere (Figure S8). In one third of the samples, such an increase can be expected to exceed a factor of 10 under daylight conditions. Even in the one third of the samples that did not show clear signs of atmospheric CCN production, the observed primary emissions of CCN-sized particles appear to be twice as high as previously indicated [*Janhäll et al.*, 2010]. During the initial aging, the $\Delta\omega$ will exceed 0.65 in approximately 90% of the samples, whereas the remaining 10% of observed biomass burning plume aerosol will have a heating effect over grassland. These observations have major implications for understanding the climatic effects of biomass burning aerosols, since the aging processes take place over spatial and temporal scales that are neither covered by emission inventories nor captured by large-scale model simulations.

References

Abel, S. J., J. M. Haywood, E. J. Highwood, J. Li, and P. R. Buseck (2003), Evolution of biomass burning aerosol properties from an agricultural fire in southern Africa, *Geophys. Res. Lett.*, *30*(15), 1783, doi:10.1029/2003GL017342.

Adler, G., J. M. Flores, A. Abo Riziq, S. Borrmann, and Y. Rudich (2011), Chemical, physical, and optical evolution of biomass burning aerosols: A case study, *Atmos. Chem. Phys.*, *11*(4), 1491–1503, doi:10.5194/acp-11-1491-2011.

Akagi, S. K., R. J. Yokelson, C. Wiedinmyer, M. J. Alvarado, J. S. Reid, T. Karl, J. D. Crounse, and P. O. Wennberg (2011), Emission factors for open and domestic biomass burning for use in atmospheric models, *Atmos. Chem. Phys.*, *11*(9), 4039–4072, doi:10.5194/acp-11-4039-2011.

Akagi, S. K., et al. (2012), Evolution of trace gases and particles emitted by a chaparral fire in California, *Atmos. Chem. Phys.*, *12*(3), 1397–1421, doi:10.5194/acp-12-1397-2012.

Andreae, M. O., and P. Merlet (2001), Emission of trace gases and aerosols from biomass burning, *Global Biogeochem. Cycles*, *15*(4), 955–966, doi:10.1029/2000GB001382.

Andreae, M. O., and D. Rosenfeld (2008), Aerosol-cloud-precipitation interactions. Part 1. The nature and sources of cloud-active aerosols, *Earth Sci. Rev.*, *89*(1–2), 13–41, doi:10.1016/j.earscirev.2008.03.001.

Belward, A. S., J. E. Estes, and K. D. Kline (1999), The IGBP-DIS global 1-km land-cover data set DISCover: A project overview, *Photogramm. Eng. Remote Sens.*, *65*(9), 1013–1020.

Bond, T. C., et al. (2013), Bounding the role of black carbon in the climate system: A scientific assessment, *J. Geophys. Res. Atmos.*, *118*, 5380–5552, doi:10.1002/jgrd.50171.

Capes, G., B. Johnson, G. McFiggans, P. I. Williams, J. Haywood, and H. Coe (2008), Aging of biomass burning aerosols over West Africa: Aircraft measurements of chemical composition, microphysical properties, and emission ratios, *J. Geophys. Res.*, *113*, D00C15, doi:10.1029/2008JD009845.

Chen, L.-W. A., H. Moosmüller, W. P. Arnott, J. C. Chow, J. G. Watson, R. A. Susott, R. E. Babbitt, C. E. Wold, E. N. Lincoln, and W. M. Hao (2006), Particle emissions from laboratory combustion of wildland fuels: In situ optical and mass measurements, *Geophys. Res. Lett.*, *33*, L04803, doi:10.1029/2005GL024838.

Christian, T. J., B. Kleiss, R. J. Yokelson, R. Holzinger, P. J. Crutzen, W. M. Hao, B. H. Saharjo, and D. E. Ward (2003), Comprehensive laboratory measurements of biomass-burning emissions: 1. Emissions from Indonesian, African, and other fuels, *J. Geophys. Res.*, *108*(D23), 4719, doi:10.1029/2003JD003704.

Cubison, M. J., et al. (2011), Effects of aging on organic aerosol from open biomass burning smoke in aircraft and laboratory studies, *Atmos. Chem. Phys.*, *11*(23), 12,049–12,064, doi:10.5194/acp-11-12049-2011.

Engelhart, G. J., C. J. Hennigan, M. A. Miracolo, A. L. Robinson, and S. N. Pandis (2012), Cloud condensation nuclei activity of fresh primary and aged biomass burning aerosol, *Atmos. Chem. Phys.*, *12*(15), 7285–7293, doi:10.5194/acp-12-7285-2012.

Formenti, P., W. Elbert, W. Maenhaut, J. Haywood, S. Osborne, and M. O. Andreae (2003), Inorganic and carbonaceous aerosols during the Southern African Regional Science Initiative (SAFARI 2000) experiment: Chemical characteristics, physical properties, and emission data for smoke from African biomass burning, *J. Geophys. Res.*, *108*(D13), 8488, doi:10.1029/2002JD002408.

Friedl, M. A., et al. (2002), Global land cover mapping from MODIS: Algorithms and early results, *Remote Sens. Environ.*, *83*(1–2), 287–302, doi:10.1016/S0034-4257(02)00078-0.

Friedl, M. A., D. Sulla-Menashe, B. Tan, A. Schneider, N. Ramankutty, A. Sibley, and X. Huang (2010), MODIS Collection 5 global land cover: Algorithm refinements and characterization of new datasets, *Remote Sens. Environ.*, *114*(1), 168–182, doi:10.1016/j.rse.2009.08.016.

Gao, F., C. B. Schaaf, A. H. Strahler, A. Roesch, W. Lucht, and R. Dickinson (2005), MODIS bidirectional reflectance distribution function and albedo Climate Modeling Grid products and the variability of albedo for major global vegetation types, *J. Geophys. Res.*, *110*, D01104, doi:10.1029/2004JD005190.

Giglio, L. (2007), Characterization of the tropical diurnal fire cycle using VIRS and MODIS observations, *Remote Sens. Environ.*, *108*, 407–421, doi:10.1016/j.rse.2006.11.018.

Grieshop, A. P., N. M. Donahue, and A. L. Robinson (2009a), Laboratory investigation of photochemical oxidation of organic aerosol from wood fires 2: Analysis of aerosol mass spectrometer data, *Atmos. Chem. Phys.*, *9*(6), 2227–2240, doi:10.5194/acp-9-2227-2009.

Grieshop, A. P., J. M. Logue, N. M. Donahue, and A. L. Robinson (2009b), Laboratory investigation of photochemical oxidation of organic aerosol from wood fires 1: Measurement and simulation of organic aerosol evolution, *Atmos. Chem. Phys.*, *9*(4), 1263–1277, doi:10.5194/acp-9-1263-2009.

Hennigan, C. J., et al. (2011), Chemical and physical transformations of organic aerosol from the photo-oxidation of open biomass burning emissions in an environmental chamber, *Atmos. Chem. Phys.*, *11*(15), 7669–7686, doi:10.5194/acp-11-7669-2011.

Hennigan, C. J., D. M. Westervelt, I. Riipinen, G. J. Engelhart, T. Lee, J. L. Collett, S. N. Pandis, P. J. Adams, and A. L. Robinson (2012), New particle formation and growth in biomass burning plumes: An important source of cloud condensation nuclei, *Geophys. Res. Lett.*, *39*, L09805, doi:10.1029/2012GL050930.

Hobbs, P. V., P. Sinha, R. J. Yokelson, T. J. Christian, D. R. Blake, S. Gao, T. W. Kirchstetter, T. Novakov, and P. Pilewskie (2003), Evolution of gases and particles from a savanna fire in South Africa, *J. Geophys. Res.*, *108*(D13), 8485, doi:10.1029/2002JD002352.

Janhäll, S., M. O. Andreae, and U. Pöschl (2010), Biomass burning aerosol emissions from vegetation fires: Particle number and mass emission factors and size distributions, *Atmos. Chem. Phys.*, *10*(3), 1427–1439, doi:10.5194/acp-10-1427-2010.

Kerminen, V.-M., K. E. J. Lehtinen, T. Anttila, and M. Kulmala (2004), Dynamics of atmospheric nucleation mode particles: A timescale analysis, *Tellus*, *56B*, 135–146.

Kerminen, V.-M., et al. (2012), Cloud condensation nuclei production associated with atmospheric nucleation: A synthesis based on existing literature and new results, *Atmos. Chem. Phys.*, *12*(24), 12,037–12,059, doi:10.5194/acp-12-12037-2012.

King, M. D., Y. J. Kaufman, D. Tanré, and T. Nakajima (1999), Remote sensing of tropospheric aerosols from space: Past, present, and future, *Bull. Am. Meteorol. Soc.*, *80*, 2229–2259.

Lack, D. A., J. M. Langridge, R. Bahreini, C. D. Cappa, A. M. Middlebrook, and J. P. Schwarz (2012), Brown carbon and internal mixing in biomass burning particles, *Proc. Natl. Acad. Sci. U.S.A.*, *109*(37), 14,802–14,807, doi:10.1073/pnas.1206575109.

Lack, D. A., R. Bahreni, J. M. Langridge, J. B. Gilman, and A. M. Middlebrook (2013), Brown carbon absorption linked to organic mass tracers in biomass burning particles, *Atmos. Chem. Phys.*, *13*(5), 2415–2422, doi:10.5194/acp-13-2415-2013.

Langmann, B., B. Duncan, C. Textor, J. Trentmann, and G. R. van der Werf (2009), Vegetation fire emissions and their impact on air pollution and climate, *Atmos. Environ.*, *43*(1), 107–116, doi:10.1016/j.atmosenv.2008.09.047.

Leahy, L. V., T. L. Anderson, T. F. Eck, and R. W. Bergstrom (2007), A synthesis of single scattering albedo of biomass burning aerosol over southern Africa during SAFARI 2000, *Geophys. Res. Lett.*, *34*, L12814, doi:10.1029/2007GL029697.

Le Canut, P., M. Andreae, G. Harris, F. Wienhold, and T. Zenker (1996), Airborne studies of emissions from savanna fires in southern Africa. 1. Aerosol emissions measured with a laser optical particle counter, *J. Geophys. Res.*, *101*(D19), 23,615–23,630, doi:10.1029/95JD02610.

Lewis, K., W. P. Arnott, H. Moosmüller, and C. E. Wold (2008), Strong spectral variation of biomass smoke light absorption and single scattering albedo observed with a novel dual-wavelength photoacoustic instrument, *J. Geophys. Res.*, *113*, D16203, doi:10.1029/2007JD009699.

Liu, S., et al. (2013), Aerosol single scattering albedo dependence on biomass combustion efficiency: Laboratory and field studies, *Geophysical Research Letters*, *41*, 742–748, doi:10.1002/2013GL058392.

Mao, J., L. W. Horowitz, V. Naik, S. Fan, J. Liu, and A. M. Fiore (2013), Sensitivity of tropospheric oxidants to biomass burning emissions: Implications for radiative forcing, *Geophys. Res. Lett.*, *40*, 1241–1246, doi:10.1002/grl.50210.

Massoli, P., et al. (2010), Relationship between aerosol oxidation level and hygroscopic properties of laboratory generated secondary organic aerosol (SOA) particles, *Geophys. Res. Lett.*, *37*, L24801, doi:10.1029/2010GL045258.

Ng, N. L., et al. (2011), An Aerosol Chemical Speciation Monitor (ACSM) for routine monitoring of the composition and mass concentrations of ambient aerosol, *Aerosol Sci. Technol.*, *45*(7), 780–794, doi:10.1080/02786826.2011.560211.

Ortega, A. M., D. A. Day, M. J. Cubison, W. H. Brune, D. Bon, J. A. de Gouw, and J. L. Jimenez (2013), Secondary organic aerosol formation and primary organic aerosol oxidation from biomass-burning smoke in a flow reactor during FLAME-3, *Atmos. Chem. Phys.*, *13*(22), 11,551–11,571, doi:10.5194/acp-13-11551-2013.

Petäjä, T., et al. (2013), Transportable aerosol characterization trailer with trace gas chemistry: Design, instruments and verification, *Aerosol Air Qual. Res.*, *13*(2), 421–435, doi:10.4209/aaqr.2012.08.0207.

Reid, J. S., and P. V. Hobbs (1998), Physical and optical properties of young smoke from individual biomass fires in Brazil, *J. Geophys. Res.*, *103*(D24), 32,013–32,030, doi:10.1029/98JD00159.

Reid, J. S., R. Koppmann, T. F. Eck, and D. P. Eleuterio (2005a), A review of biomass burning emissions part II: Intensive physical properties of biomass burning particles, *Atmos. Chem. Phys.*, *5*(3), 799–825, doi:10.5194/acp-5-799-2005.

Reid, J. S., T. F. Eck, S. A. Christopher, R. Koppmann, O. Dubovik, D. P. Eleuterio, B. N. Holben, E. A. Reid, and J. Zhang (2005b), A review of biomass burning emissions part III: Intensive optical properties of biomass burning particles, *Atmos. Chem. Phys.*, *5*(3), 827–849, doi:10.5194/acp-5-827-2005.

Roy, D. P., L. Boschetti, C. O. Justice, and J. Ju (2008), The collection 5 MODIS burned area product—Global evaluation by comparison with the MODIS active fire product, *Remote Sens. Environ.*, *112*(9), 3690–3707, doi:10.1016/j.rse.2008.05.013.

Scepan, J. (1999), Thematic validation of high-resolution global land-cover data sets, *Photogramm. Eng. Remote Sens.*, *65*(9), 1051–1060.

Spracklen, D. V., K. S. Carslaw, U. Pöschl, A. Rap, and P. M. Forster (2011), Global cloud condensation nuclei influenced by carbonaceous combustion aerosol, *Atmos. Chem. Phys.*, *11*(17), 9067–9087, doi:10.5194/acp-11-9067-2011.

van der Werf, G. R., J. T. Randerson, L. Giglio, G. J. Collatz, M. Mu, P. S. Kasibhatla, D. C. Morton, R. S. DeFries, Y. Jin, and T. T. van Leeuwen (2010), Global fire emissions and the contribution of deforestation, savanna, forest, agricultural, and peat fires (1997–2009), *Atmos. Chem. Phys.*, *10*(23), 11,707–11,735, doi:10.5194/acp-10-11707-2010.

Yokelson, R. J., et al. (2009), Emissions from biomass burning in the Yucatan, *Atmos. Chem. Phys.*, *9*(15), 5785–5812, doi:10.5194/acp-9-5785-2009.

Yokelson, R. J., et al. (2013), Coupling field and laboratory measurements to estimate the emission factors of identified and unidentified trace gases for prescribed fires, *Atmos. Chem. Phys.*, *13*(1), 89–116, doi:10.5194/acp-13-89-2013.